DOI: 10.61782/fa.2025.0462

FORUM ACUSTICUM
EURONOISE 2025

IMPROVEMENTS IN MEASURING ACOUSTIC IMPEDANCE OF OUTDOOR GROUND SURFACES

Andreas Fuchs **Manfred Haider**
AIT Austrian Institute of Technology GmbH, Transportation Infrastructure Technologies.

ABSTRACT

The acoustic impedance of a ground surface has an influence on sound propagation over long distances and therefore needs to be known to predict the sound imissions for residents suffering from transport noise. In the Commission Directive (EU) 2015/996 (CNOSSOS-EU) as well as in more detailed methods (e.g. NORD2000), a classification of flow resistivity is given for various ground surfaces. In Nordtest NT ACOU 104:1999 a suitable measurement method for measuring ground surface absorption is described. In this work, the setup of NT ACOU 104 is combined with modern approaches to signal processing and analysis. Quarterly measurements were carried out at eight locations in which the impulse responses between the loudspeaker and microphones were measured. In analyzing the measurements, the ground surface's effective flow resisitivty was calculated using least-squares optimization, and various impedance models were investigated for appropriability. The performance of the different impedance models was evaluated by predicting the sound pressure of a third additionally measured microphone position.

Keywords: *acoustic impedance, ground surface, measurement*

1. INTRODUCTION

The study of the interaction between airborne sound and a surface has many applications, e.g. noise abatement in machines or room acoustics. Especially for understanding outdoor sound propagation the interaction with the ground surface must be well understood.

In the Commission Directive (EU) 2015/996 (CNOSSOS-EU) the ground surface is categorized in eight categories, where the acoustic absorption properties of the ground are mainly linked to its porosity [1]. The eight categories of CNOSSOS-EU extend the seven *impedance classes* of the HARMONOISE model [2], which is considered overall to be more elaborate and in complex and more realistic situations superior to the NMPB 2008 model [3], which is the basis for CNOSSOS-EU. Table 1 lists the eight categories of ground surfaces. In CNOSSOS-EU a factor G is used, which controls the amount of absorption of the surface. In the sound propagation model HARMONOISE as well as in the similar NORD2000 [4], the ground impedance class is expressed by a effective flow resistivity σ_e, which is used as an input factor for calculating the surface impedance with the empirical Delany-Bazley model. HARMONOISE and NORD2000 only use seven classes and make no distinction between the classes G and H. [1]

For the determination of the effective flow resistivity NORD2000 refers to the Nordtest method NT ACOU 104 [5], which devides the acoustic impedance of ground surfaces into twelve flow resistivity classes using the Delany-Bazley impedance model. For many research questions, a precise prediction of outdoor sound propagation is mandatory, if a reliable determination of the acoustic ground surface for the NORD2000 or HARMONOISE models is necessary. As the latest version of NT ACOU 104 dates back to 1999, more modern approaches to signal processing and analysis are examined in this paper.

*Corresponding author: andreas.fuchs@ait.ac.at.

[1] For a hard surface HARMONOISE suggests a flow resistivity of 200 000 kPa s m^{-2} whereas NORD2000 suggests a flow resistivity of 20 000 kPa s m^{-2}.

Table 1: Ground impedance classes with factor G (CNOSSOS-EU) and effective flow resistivity σ_e (HARMONOISE).

	Description	G	σ_e (kPa s m^{-2})
A	Very soft (snow or moss-like)	1	12.5
B	Soft forest floor (short, dense heather-like or thick moss)	1	31.5
C	Uncompacted, loose ground (forest floors, pasture field)	1	80
D	Normal uncompacted ground (forest floors, pasture field)	1	200
E	Compacted field and gravel	0.7	500
F	Compacted dense ground (gravel road, parking lot)	0.3	2000
G	Hard surfaces (mostly normal asphalt, concrete)	0	20 000
H	Very hard and dense surfaces (dense asphalt, concrete, water)	0	200 000

2. MEASUREMENT OF GROUND SURFACE IMPEDANCE

This section gives a short summary of the NT ACOU 104 test method. Afterwards, the studied alterations are presented.

2.1 NT ACOU 104

The nordtest method NT ACOU 104 measures the level difference in third-octave bands between two microphones above a ground surface [5]. The set-up of the microphones and loudspeaker is shown in Fig. 1. The test signal shall consist of a broadband random or pseudo random noise and the time-averaged sound pressure level over at least 15 seconds is recorded for each third-octave band j in the frequency range from 200 Hz to 2500 Hz. The measured level difference

$$\Delta L_{i,j}^{\mathrm{M}} = L_{\mathrm{eq},i,j,\mathrm{top}} - L_{\mathrm{eq},i,j,\mathrm{bottom}} \qquad (1)$$

is recorded and averaged over four independent measurements i of an adjacent piece of identical ground to calculate ΔL_j^{M}.

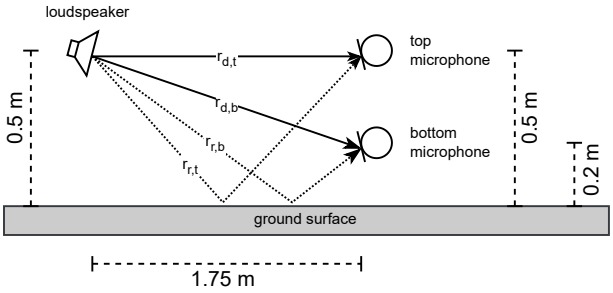

Figure 1: Measurement set-up according to NT ACOU 104.

This measured and averaged level difference ΔL_j^{M} is compared to precalculated level differences $\Delta L_j^{\mathrm{C}}(x)$ for distinct classes of flow resistivity, where the class with the smallest linear error is selected as flow resistivity. For a general parameter x, which might be multi-dimensional, this minimization can be written as:

$$\min_x E(x), \quad E(x) = \sum_j \left|\Delta L_j^{\mathrm{M}} - \Delta L_j^{\mathrm{C}}(x)\right| \qquad (2)$$

In NT ACOU 104, values are given in tables for $\Delta L_j^{\mathrm{C}}(x)$ for twelve different flow resistivity classes for a single-layer Delany-Bazley impedance model, as well as for a porous layer above a rigid surface with 0.05 m, 0.1 m and 0.15 m thickness for high and low temperatures. For measurements to be valid, the standard deviation between the repeated measurements for each third-octave band $s_{\mathrm{D},j}$ shall not exceed 4 dB. Also, the error E should be less than 15 dB. In an informative annex in NT ACOU 104 the use of a different impedance model is described.

2.2 Proposed adaptions to NT ACOU 104

The following adaptions to NT ACOU 104 are proposed and presented in this section:

- record impulse responses with time windowing,
- always solve the minimization problem for continuous values,
- examine different impedance models
- validate best fit with third microphone position.

2.2.1 Record impulse responses and use time-windowing

Recording broadband noise is sensitive to disturbing noise sources, wind noise and the surrounding area. For the in-situ measurement of the intrinsic characteristics of sound

reflection of noise barriers under direct sound field conditions (as described in EN 1793-5 [6]), impulse responses are used to measure the reflection index of noise barriers and the measurements can be performed along a highway under normal operation. If a Maximum-Length-Sequence (MLS) is used as test signal for NT ACOU 104 to calculate the impulse responses, this technically still classifies as a pseudo random test signal. This adds robustness against disturbing noise sources for the measurements. However, another advantage of impulse responses is the possibility to perform time filtering to suppress unwanted reflections. Beside the calculation of an impulse response, we propose the use of the Adrienne time-window from EN 1793-5 [6] with a length of the flat top (main part) of 10 ms and total window length of 14.8 ms. Therefore, a third-octave band level can be calculated for a impulse response $h(t)$, a time window $w_\mathrm{A}(t)$ and the Fourier transform $\mathcal{F}$ with

$$L_j = 10\log\left(\int_{\Delta f_j} |\mathcal{F}[h(t)w_\mathrm{A}(t)]|^2\right) \tag{3}$$

for the third-octave frequency bands j with a width of Δf_j. Figure 2 shows the measured impulse response for the top microphone over grass (green line) as well as the proposed Adrienne time window (orange line). At around 5.1 ms the first peak of the direct path is visible, whereas at 6 ms the first peak of the reflected component can be distinguished. The time window is long enough to include the whole impulse response of the loudspeaker for both components.

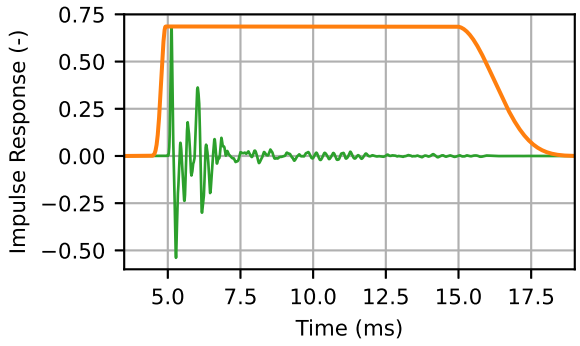

Figure 2: Impulse response (green) and Adrienne time window (orange).

2.2.2 *Solving the minimization problem for continuous values*

Instead of a table look-up from NT ACOU 104 we suggest solving the minimization problem for continuous values of the required impedance parameter(s). This can be achieved with the underlying Weyl-Van der Pol equation, which is able to predict the sound pressure p from a point source above a locally reacting ground as a superposition of the sound pressure from the direct path p_d and the reflected path (p_r), which is multiplied with the *spherical reflection coefficient* Q [7]:

$$p = p_\mathrm{d} + Qp_\mathrm{r} = \frac{\mathrm{e}^{\mathrm{i}kr_d}}{4\pi r_d} + Q\frac{\mathrm{e}^{\mathrm{i}kr_r}}{4\pi r_r}, \tag{4a}$$

$$Q = R_\mathrm{p} + (1-R_\mathrm{p})(1+\mathrm{i}\sqrt{\pi}w\mathrm{e}^{-w^2}\,\mathrm{erf}(-\mathrm{i}w)), \tag{4b}$$

$$w = \frac{1+\mathrm{i}}{2}\sqrt{kr_r}(\cos(\theta)+Z^{-1}), \tag{4c}$$

$$R_\mathrm{p} = \frac{\cos(\theta)-Z^{-1}}{\cos(\theta)+Z^{-1}} \tag{4d}$$

and R_p as the plane wave reflection coefficient of the locally reacting ground surface, r_d and r_r as the distance between source and receiver position for the direct and reflected path respectively, the wave number k, the incident angle θ and the normalized impedance of the ground Z. If the Delany-Bazley impedance model is used, then the impedance is calculated with [5]

$$Z = 1 + 9.08\left(\frac{f}{\sigma_\mathrm{e}}\right)^{-0.75} + i11.9\left(\frac{f}{\sigma_\mathrm{e}}\right)^{-0.73}. \tag{5}$$

The predicted sound pressure levels must be calculated in third-octave bands for both microphone positions for comparison with the measurement data. Afterwards, the minimization in Eqn. (2) can be solved for continuous values of the required impedance parameter.

2.2.3 *Examination of different impedance models*

Including the Annex D, NT ACOU 104 suggests the use of three different impedance models: Delany-Bazley, Delany-Bazley with an additional porous layer above a rigid surface and the variable porosity model. Among the commonly used impedance models models [8], [9], we studied the following ones by using the respective model in the plane wave reflection coefficient in Eqn. (4d):

Delany-Bazley The semi-empirical Delany-Bazley [8] model given in Eqn. (5) with the parameter effective flow resistivity σ_e.

Variable Porosity The variable porosity model considers an increasing porosity with increasing depth as approximation with two parameters (effective flow resistivity σ_e and effective rate of change of porosity α_e) and uses the heat capacity ratio γ [7]:

$$Z = \frac{1+\mathrm{i}}{\sqrt{\pi\gamma\rho_0}}\sqrt{\frac{\sigma_\mathrm{e}}{f}} + \frac{\mathrm{i}c_0\alpha_\mathrm{e}}{8\pi\gamma f}. \tag{6}$$

Zwikker-Kosten The phenomenological model from Zwikker-Kosten uses the three parameters flow resistivity σ, porosity Ω and structure factor K [7]:

$$Z = \frac{\sqrt{K}}{\Omega}\left(1 + \frac{\mathrm{i}\Omega\sigma}{2\pi f\rho_0 K}\right). \tag{7}$$

Taraldsen Taraldsen transformed the phenomenological model from Zwicker-Kosten to a one-parameter model (effective flow resistivity σ_e) [7]:

$$Z = \left[\sqrt{\gamma}\frac{\Omega}{\sqrt{T}}\left(1 + \frac{f*}{f}\right)\right]^{-1} \tag{8a}$$

$$f* = \frac{1}{2\pi\rho_0}\frac{\Omega}{\sqrt{T}}\sigma_\mathrm{e} \tag{8b}$$

$$\frac{\Omega}{\sqrt{T}} = 100\left(10^{X/10}\right) \tag{8c}$$

$$X = \frac{1}{19.76}\Big[-10\log(\sigma_\mathrm{e}) + 404.55 + \sqrt{546.166 + [9.35 - 10\log(\sigma_\mathrm{e})]^2}\Big]. \tag{8d}$$

Slit-pore The slit-pore model is based on the simulation of the internal structure of the absorber with interconnected slits and pores. For the impedance of the ground, the assumption of identically wound slit-like pores is used with the three parameters flow resistivity σ, porosity Ω and tortuosity T [8] and uses the Prandtl number Pr:

$$Z = \frac{1}{\rho_0 c_0}\sqrt{\frac{T}{\Omega^2}\frac{\rho(\lambda)}{C(\lambda)}} \tag{9a}$$

$$\rho(\lambda) = \frac{\rho_0}{G_S(\lambda)} \tag{9b}$$

$$C(\lambda) = \frac{1}{\gamma P_0}\left[\gamma - (\gamma-1)G_S(\lambda\sqrt{Pr})\right] \tag{9c}$$

$$G_S(\lambda) = 1 - \frac{\tanh(\lambda\sqrt{-\mathrm{i}})}{\lambda\sqrt{-\mathrm{i}}} \tag{9d}$$

$$\lambda = \sqrt{\frac{6\rho_0\pi f T}{\Omega\sigma}} \tag{9e}$$

For the Delany-Bazley, the Zwikker-Kosten as well as for the slit-pore model also the respective layered model is considered, where the impedance is calculated with

$$Z = Z_\mathrm{n}\coth(-ikd) \tag{10}$$

with the layer thickness d of the porous material over a rigid surface. Z_n is the impedance of the according impedance model (Eqn. (5), (7) or (9a) respectively).

2.2.4 *Validate best fit with third microphone position*

For validation purposes, we propose to measure a third microphone position between the top and bottom microphone in the set-up of NT ACOU 104 (see Fig. 1), which is 35 cm above the ground. The *validation* level difference $\Delta L^\mathrm{M}_{\mathrm{v},j}$ is calculated from the difference from the validation to the bottom microphone via Eqn. (4a) and Eqn. (1). This gives the advantage of new independent measurement data on an identical test specimen with minimal extra effort. The *validation error* E_v is then similar to Eqn. (2)

$$E_\mathrm{v} = \sum_j \left|\Delta L^\mathrm{M}_{\mathrm{v},j} - \Delta L^\mathrm{C}_{\mathrm{v},j}(x)\right|. \tag{11}$$

Figure 3 shows the level difference ΔL_j for the standard set-up from NT ACOU 104 (top to bottom microphone) as well as as the level difference from the additional proposed validation microphone to the bottom microphone $\Delta L_{\mathrm{v},j}$. The computed level difference values are calculated for a flow resistivity class of 400 kPa s m^{-2},

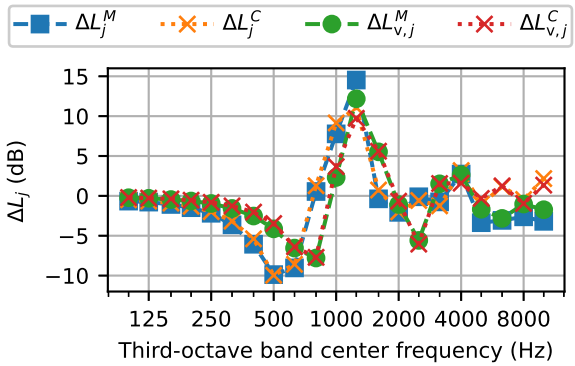

Figure 3: Measured ($^\mathrm{M}$) and computed ($^\mathrm{C}$) level difference between the top and bottom microphone (ΔL_j) and additional validation microphone and bottom ($\Delta L_{\mathrm{v},j}$).

which was calculated for a minimum error of E (Eqn. (2)). For the additional validation microphone the third-octave band values of the level difference $\Delta L_{\mathrm{v},j}$ are different to ΔL_j due to the changed geometry. Nevertheless, the computed values are quite close to the measured values for a frequency range from 100 Hz to 4000 Hz. This gives the ability to validate the obtained value of $\sigma_\mathrm{e} = 400\,\mathrm{kPa\,s\,m^{-2}}$ for a microphone and geometry, which was not included in the calculation of the value.

3. MEASUREMENTS

The analysis presented in this paper is based on measurements which were performed to study the ground surface absorption of earth berms for calculating sound propagation alongside highways. Therefore, measurements were performed on flat and inclined surfaces, although NT ACOU 104 suggests only to perform measurements on a flat surface. For the measurements on the slope, the set-up according to NT ACOU 104 is rotated with respect to the inclination. Measurements were performed on two sites, with multiple measurement positions for each site:

Site A: 2 measurement positions on level ground and 4 measurement positions on tilted surfaces with angles ±16° and ±35°. [2]

Site B: 2 measurement positions on tilted surfaces with angles 35° and 38°.

The measurements were performed repeatedly on the same spots on a quarter year basis from Q4 2023 until Q3 2024. Although, all measurements sites can be considered covered with grass, the ground was much more compacted in Q4 2023. In Q1 2024 and Q3 2024 very similar conditions could be found with low length grass, where in Q2 2024 the measurements were performed on a hot day with high grass. The measurement sites are less than 30 km apart from each other. Figure 4 to Fig. 7 show pictures of the measurement sites. As this study did not focus on performing measurements, the variation of the measurement sites is limited. Nevertheless, the data set spans over four of the seven impedance classes of HARMONOISE (classes B - E from Tab. 1).

For the measurements a MLS signal was used as test signal with a length of two seconds, which was repeated

[2] For a positive angle the loudspeaker is below the microphone and emits sound upwards the slope, whereas for a negative angle the loudspeaker is placed above the microphones.

Figure 4: Picture of measurement site A Q4 2023.

Figure 5: Picture of measurement site A Q2 2024.

Figure 6: Picture of measurement site B Q4 2023.

Figure 7: Picture of measurement site B Q2 2024.

30 times. Therefore, it is possible to calculate a two second long impulse response for each microphone, which was averaged 30 times.

4. RESULTS AND DISCUSSION

In this section the proposed adaptions to NT ACOU 104 from section 2.2 are evaluated.

4.1 Solving the minimization problem

The minimization problem in Eqn. (2) is solved using a curve-fitting algorithm. This gives the ability to calculate continuous values for the impedance model parameters, especially a continuous value for the effective flow resisitivty for the Delany-Bazley model instead of the 12 classes according to NT ACOU 104. Figure 8 shows a box plot of the error E from Eqn. (2) and validation error E_v from Eqn. (11) for all obtained measurements, if the effective flow resisitivty, which minimizes E, is determined with a table lookup as in NT ACOU 104 or if a continuous value is calculated. This value is then used to calculate the validation error E_v by using it to predict the level difference. Afterwards, the predicted level difference is compared to the measured level difference between the validation and bottom microphone and the validation error E_v calculated. As expected, the errors are smaller for the fitting approach compared to the table lookup method. However, the improvement can be seen even better for the validation error E_v, where the mean error is decreased by about 2 dB.

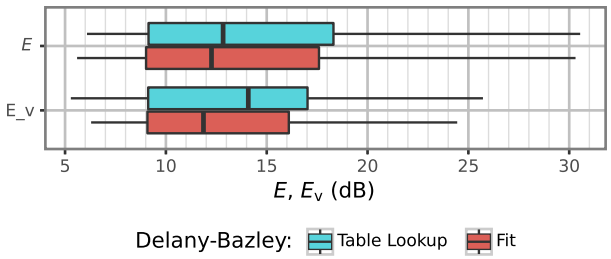

Figure 8: Comparison of the error between the measured and computed level difference for the standard set-up (E) and the validation set-up (E_v) for all obtained measurements (Delany-Bazley model).

4.2 Impulse Responses

For all performed measurements the effective flow resistivity σ_e was determined according to the Delany-Bazley model by running a curve fitting algorithm on the error function $E(x)$ (Eqn. (2)) for two specific test cases:

Noise The $L_{\mathrm{eq},j}$ values are calculated with time filters on the recorded signal and averaged over 60 s.

Impulse Response Instead of the $L_{\mathrm{eq},j}$, the L_j from Eqn. (3) are used as third-octave band levels and are calculated by deconvoluting the recorded signal to obtain the impulse response.

Figure 9 compares the effective flow resistivity σ_e for the two test cases, where no significant deviations are visible. For one measurement the deviation is 6 %, for all other measurements the deviation is less than 5 %, Also, for more than half of the 27 data points the deviation is less than 1 kPa s m^{-2}.

In the standard deviations between the four measurements for each measurement position no significant difference can be found, as the mean difference between the standard deviation for the *noise* and *impulse response* test case for each measurement position for all third-octave bands is smaller than 0.1 dB. As the measurements were performed without external noise sources, the main benefit of the impulse response calculation can not be shown. Nevertheless, the results are similar and there is no apparent downside to using impulse responses.

4.3 Impedance Models

The error E as well as the validation error E_v can also be used to compare different impedance models. Figure 10

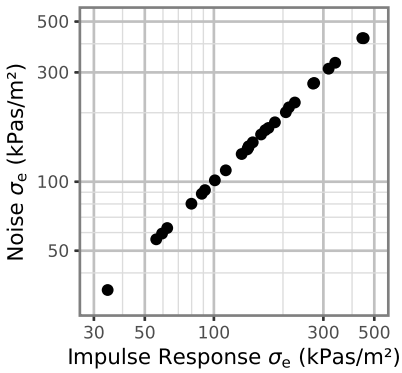

Figure 9: Estimated effective flow resistivity σ_e with the Delany-Bazley impedance model by directly processing the noise signal or calculating impulse responses.

shows box plots, where the range of the occurring errors for all obtained measurements is visible with respect to the impedance model. Again, the validation error E_v is calculated by using the obtained impedance model parameters, which result from minimizing the error E for the top to bottom microphone set-up, for predicting and comparing the level difference of the validation to bottom microphone set-up. The impedance models are ordered by increasing number of parameters from top to bottom. For the one-parameter Taraldsen model it was not possible to find a good fit. All the other newly considered models performed similar or better than the Delany-Bazley model. Especially, the variable porosity model (except for a few outliers) and also the phenomenological model from Zwikker-Kosten show promising results pushing the mean of the errors in the dataset closer to 10 dB than the Delany-Bazley model. However, the Delany-Bazley model shows a quite reasonable performance considering its simplicity. The respective layer variants of the models show small improvements, but might not be applicable for the performed measurements. The validation error E_v is in the same range as E except for the Taraldsen impedance model, which supports the assumption that the fit of the these models can be generalized and can be used for sound propagation calculations.

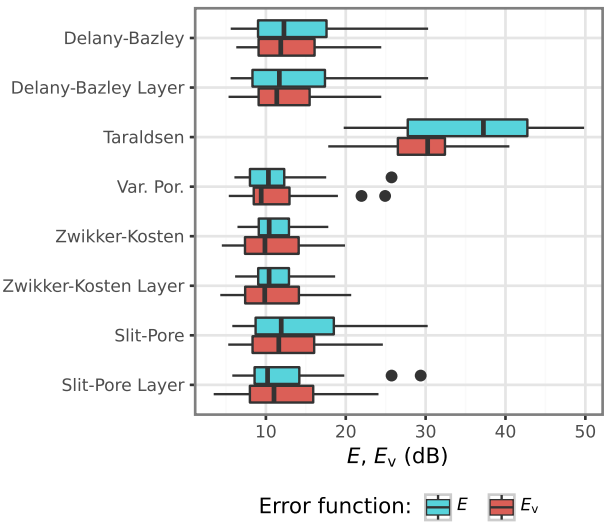

Figure 10: Comparison of error E and validation error E_v of the impedance models for all obtained measurements.

4.4 Influence of Angle

In contrast to NT ACOU 104, measurements were also performed on tilted surfaces. No significant influence of the angle of the surface on the error and the validation error could be found, which means the fit to the standard set-up and the validation set-up works for tilted surfaces as well as for flat ground. Nevertheless, the obtained values for the flow resistivity are quite different for the different angles. Figure 11 shows the estimated effective flow resis-

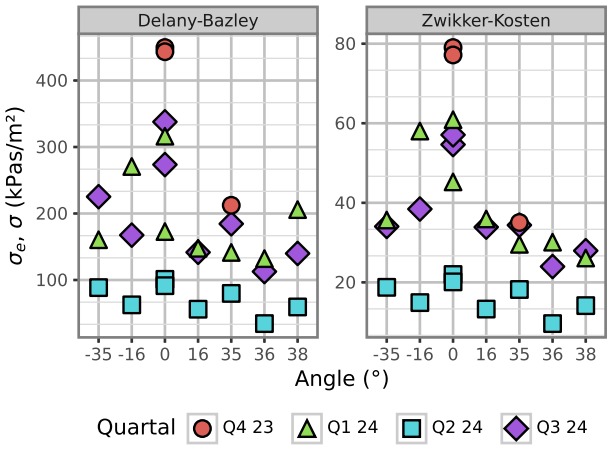

Figure 11: Estimated (effective) flow resistivity for the Delany-Bazley (σ_e) and the Zwikker-Kosten (σ) model for all obtained measurements.

tivity σ_e for the Delany-Bazley impedance model as well as the flow resistivity σ for the Zwikker-Kosten model for all measurements for the different surface angles for the repeated measurements. It can be seen, that the flow resistivity is significantly lower in Q2 2024, which may be attributed to a drier ground. This can also be attributed to the porosity Ω in the Zwikker-Kosten model, which is significantly higher in Q2 2024 than for the other quarters. For Q4 2023 not all measurements were performed. Nevertheless, the respective highest values for the flow resistivity were measured in this quarter, which get close to class E according to the HARMONOISE classification (compacted field). For the measurements, which were not performed in Q2 2024, it can be seen that for the non flat measurements the estimated flow resistivity is lower. This may be attributed to a less compacted ground on the earth berm. It should be noted, that the measurements at 36° and 38° inclination were performed at a different site, which might have different sound absorbing characteristics.

5. SUMMARY AND OUTLOOK

In this paper, adaptions to the standard NT ACOU 104 for measuring ground surface absorption were presented. The measurements were obtained on grass covered earth berms. The use of a third microphone for validation provides valuable insight into how well the estimated parameters can actually describe the acoustic properties of the ground surface. Because the extra effort seems reasonable compared to the information gain, we recommend the use of an extra microphone position. Also, no significant difference in the analysis with impulse responses to the previous method could be found. As the measurement with impulse responses is generally seen as more robust, we encourage their use instead of evaluating noise signals.

Depending on the application, the use of a fitting algorithm to determine a continuous parameter as well as other impedance models, might improve sound propagation over long distances. Nevertheless, this must be supported by the underlying sound propagation calculation method and must be evaluated in further research. Also, the measurement on inclined surfaces showed promising results over short distances due to the low validation error. However, further research is encouraged to evaluate if for larger propagation paths it is more beneficial to use values obtained from the inclined plane than from the flat surface.

6. ACKNOWLEDGMENTS

This report is based on parts of the research project carried out at the request of the Federal Ministry for Digital and Transport, represented by the Federal Highway and Transport Research Institute, under research project No. 02.0455/2022. The author is solely responsible for the content.

7. REFERENCES

[1] Commission Directive (EU) 2015/996 of 19 May 2015 establishing common noise assessment methods according to Directive 2002/49/EC of the European Parliament and of the Council (CNOSSOS-EU), 2015.

[2] R. Nota, R. Barelds, and D. van Maercke, *Technical Report HAR32TR-040922-DGMR20, Harmonoise WP 3 Engineering method for road traffic and railway noise after validation and fine-tuning. Deliverable 18*, 2005.

[3] S. Kephalopoulos et al., "Advances in the development of common noise assessment methods in Europe: The CNOSSOS-EU framework for strategic environmental noise mapping," *Science of The Total Environment*, vol. 482-483, pp. 400–410, 2014.

[4] NORD 2000, *Comprehensive Outdoor Sound Propagation Model. Part 1: Propagation in an Atmosphere without Significant Refraction.* DELTA - Danish Electronics, Light & Acoustics, Denmark, 2001.

[5] NT ACOU 104, *Ground surfaces: Determination of the acoustic impedance - nordtest method*. Nordtest, Finland, 1999.

[6] EN 1793-5, *Road traffic noise reducing devices – Test method for determining the acoustic performance – Part 5: Intrinsic characteristics – In situ values of sound reflection under direct sound field conditions*, 2016.

[7] K. Attenborough and T. van Renterghem, *Predicting Outdoor Sound*. USA: CRC Press, 2nd ed., 2021.

[8] K. Attenborough, I. Bashir, and S. Taherzadeh, "Outdoor ground impedance models," *The Journal of the Acoustical Society of America*, vol. 129, pp. 2806–2819, 05 2011.

[9] K. Attenborough, "Outdoor ground impedance models," in *Euronoise Maastricht*, 2015.